Alcohol Attenuates CRF-Induced Excitatory Effects from the Extended Amygdala to Dorsostriatal Cholinergic Interneurons

Amanda Essoh[1], Himanshu Gangal[1], Zhenbo Huang[1], Ruifeng Chen[1], Xueyi Xie[1], Xuehua Wang[1], Valerie Vierkant[1], Miguel Garza[1], Lierni Ugartemendia[2], Maria E. Secci[3], Nicholas W. Gilpin[3], Nicholas J. Justice[2], Robert O. Messing[4] and Jun Wang[1] *

[1]Department of Neuroscience and Experimental Therapeutics, College of Medicine, Texas A&M University Health Science Center, Bryan, Texas 77807

[2]Center for Metabolic and Degenerative Disease, Institute of Molecular Medicine, University of Texas, Houston, Texas 77030

[3]Department of Physiology, Louisiana State University Health Sciences Center, New Orleans, Louisiana, 70112

[4]Department of Neuroscience, University of Texas, Austin, Texas, 78712

Running Title: Extended Amygdala–Striatum CRF Circuit Altered by Alcohol

Key Words: CRF and CRFR1, alcohol/ethanol, dorsal striatum, CeA, BNST, cholinergic interneuron, stress, Acetylcholine (ACh), slice electrophysiology, neurocircuit tracing

*To whom correspondence should be addressed:
Jun Wang, M.D., Ph.D.
2106 Medical Research and Education Building
8447 John Sharp Pkwy,
Bryan, TX 77807
Tel: 979-436-0389
Fax: 979-436-0086
E-mail: jwang188@tamu.edu

Pages: 34, Figures: 6, Abstract: 182 words, Introduction: 348, Discussion: 514

Abstract

Alcohol relapse is linked to corticotropin-releasing factor (CRF) signaling and is caused by dysfunction within reward pathway circuitry, yet the underlying mechanisms guiding this process remain unclear. Here, we investigated how CRF modulates cholinergic interneurons (CINs) in the dorsal striatum, a region critical for mediating cognitive flexibility and action selection. Using monosynaptic and retrograde circuit tracing, we identified direct inputs from CRF-expressing (CRF^+) neurons in the central amygdala (CeA) and bed nucleus of the stria terminalis (BNST) to dorsal striatal CINs. We showed that CINs express CRF receptor 1 (CRFR1) and established their functional connectivity with CeA/BNST CRF^+ projections. Functional recordings revealed that CRF enhanced CIN excitability and promoted acetylcholine release in the dorsal striatum. However, acute alcohol exposure and withdrawal attenuated the excitatory effect of CRF on CIN firing, suggesting a mechanism by which alcohol disrupts CRF-dependent neuromodulation. These findings uncover a novel CRF-mediated circuit linking the extended amygdala to the dorsal striatum and provide insight into how CRF and alcohol interact to impair striatal function. This work highlights CRF signaling as a potential target for uncovering the mechanism of stress-induced changes to the reward pathway.

Highlights

- Dorsal striatal CINs receive monosynaptic CRF^+ inputs from CeA and BNST neurons.
- CRFR1 is expressed in striatal CINs, and CRF^+ fibers are present in the dorsal striatum.
- CRF enhances dorsal striatal CIN activity via CRFR1 signaling.
- Acute alcohol exposure impairs CRF-induced cholinergic activity.

Significance Statement

The dorsal striatum regulates goal-directed behavior and is implicated in alcohol use disorder (AUD). Within this region, cholinergic interneurons (CINs) support cognitive flexibility and receive input from limbic areas, including the central amygdala (CeA) and bed nucleus of the stria terminalis (BNST). In this study, we identified direct projections from CRF-producing neurons in the CeA and BNST to dorsal striatal CINs, a subset of which express CRF receptor 1 (CRFR1). Electrophysiological recordings confirmed these projections provide functional input that is disrupted by acute alcohol exposure. These findings lay the groundwork for future studies on how CRF and alcohol interact to impair striatal function.

Introduction

Alcohol use disorder (AUD) is a chronic, recurring brain condition characterized by compulsive alcohol consumption, impaired control over drinking, and negative emotional states during withdrawal. Stress is a key contributor to both the development and recurrence of AUD, with stressful experiences and elevated stress hormone levels frequently precipitating relapse episodes in abstinent individuals [1-3]. An expanding body of clinical and preclinical evidence highlights the importance of stress-responsive neurocircuits in driving addiction-related behaviors, implicating neuropeptides like corticotropin releasing factor (CRF) in relapse vulnerability [4-8]. CRF is a central regulator of the stress response, coordinating hormonal and behavioral adaptations to stress through widespread action in both hypothalamic and extrahypothalamic brain regions. In addition to initiating hypothalamic-pituitary-adrenal (HPA) axis activity, CRF modulates affective and motivational processes via its action in the amygdala, bed nucleus of the stria terminalis (BNST), and other limbic structures.

Substantial evidence indicates that CRF signaling enhances drug-seeking behavior during stress and withdrawal across multiple substances of abuse, supporting its role as a critical mediator of relapse [5, 6, 9]. Despite extensive research on CRF in limbic areas, its role in the dorsal striatum—an area crucial for goal-directed learning, habit formation, and behavioral flexibility—remains less well understood [10-16]. Within this region, cholinergic interneurons (CINs) are key regulators of striatal output and acetylcholine (ACh)-mediated dopamine modulation, integrating diverse inputs and contributing to reward-based learning [17-19]. CINs are sensitive to neuromodulatory

influences, yet it is unclear whether they are directly targeted by CRF and how this interaction might be altered by alcohol exposure [20-22].

In this study, we investigated a novel CRF–CIN circuit linking the CeA and BNST to the dorsal striatum. Using monosynaptic and retrograde circuit tracing, we identified direct projections from CRF-expressing neurons to dorsal striatal CINs. CRF enhanced CIN excitability and promoted ACh release via CRFR1 receptors, but this excitatory effect was disrupted by acute alcohol exposure, indicating that alcohol interferes with CRF-dependent cholinergic modulation. These findings identify a CRF-CIN circuit that is vulnerable to alcohol-induced dysregulation, providing mechanistic insight into how stress peptides and alcohol interact to impair striatal function.

Materials and Methods

Animals

Male and female 3-4-month-old mice or rats were used in all studies. ChAT-eGFP (stock 007902), ChAT-Cre (stock 031661), Drd1a-tdTomato (D1-tdT, stock 016204), Ai32 (stock 012569), CRH-ires-CRE (stock 012704) and C57BL/6J (stock 000664) mice were purchased from The Jackson Laboratory [23-27]. All mice were backcrossed onto a C57BL/6 background. ChAT-Cre mice were crossed with D1-tdTomato mice to obtain ChAT-Cre;D1-tdTomato mice. CRF-Cre mice were crossed with ChAT-eGFP mice to generate CRF-Cre;ChAT-eGFP mice. CRF-Cre;Ai32 mice were generated in-house and crossed with ChAT-eGFP to generate triple transgenic CRF-Cre;Ai32;ChAT-eGFP mice. We used CRFR1-Cre-2A-tdTomato rats that have been validated for expression of Cre and tdTomato in CRFR1-expressing neurons [28]. We also used CRF-Cre rats that have been shown to express Cre recombinase in CRF-producing neurons in the CeA and

110 BNST [29]. We crossed CRF-Cre rats with a Cre-dependent tdTomato reporter line to
111 visualize CRF^+ neurons. Genotypes were confirmed through PCR analysis of tail DNA to
112 detect Cre or fluorescent protein genes in mice and rats (Cre for CRF-Cre, and ChAT-Cre;
113 tdTomato for D1-tdTomato; and GFP for Ai32) [30-34]. Animals were housed in a
114 temperature- and humidity-controlled vivarium with a 12-h light/dark cycle. Food and
115 water were available *ad libitum*. The Texas A&M University Institutional Animal Care and
116 Use Committee approved all animal care and experimental procedures.

117 **Reagents**

118 AAV8-Ef1a-FLEX-TVA-mCherry (lot # AV5008b), AAV8-FLEX-RG (lot # AV5005f),
119 and AAV-FLEX-Chrimson-tdTomato (lot # AV5844) were purchased from the UNC Vector
120 Core [35, 36]. AAVrg-pCAG-FLEX-eGFP-WPRE (catalog # 51502-AAVrg) was purchased
121 from Addgene [37], while EnvA-SADΔG-GFP was purchased from the Salk Institute [38].
122 Choline acetyltransferase (AB144P) antibody was purchased from Sigma [39]. ACh
123 sensor ($AAV\text{-}GRAB_{ACh4m}$) was obtained from BrainVTA [40]. CRF peptide and NBI 35695
124 (CRFR1 antagonist) were obtained from Tocris. 6,7-dinitroquinoxaline-2,3-dione (DNQX),
125 tetrodotoxin (TTX), 4-aminopyridine (4-AP), and bicuculline were also purchased from
126 Tocris.

127 **Stereotaxic virus infusion**

128 The stereotaxic virus infusion procedure was conducted as described previously
129 [30, 41, 42]. When required for the experimental design, AAV-DIO-TVA-mCherry and AAV-
130 DIO-RG were bilaterally infused into the dorsal striatum (AP: 0.38, mm, ML: ±1.55 mm,
131 DV: -2.90 mm from the Bregma) [43] of ChAT-Cre;D1-tdTomato mice (Fig. 1). Rabies-
132 GFP was infused at the same injection site three weeks later at a 10˚ angle to avoid

133 contamination of the infusion tract. Rabies-GFP virus was allowed to incubate for one
134 week. AAVrg-pCAG-FLEX-eGFP-WPRE was infused into the dorsal striatum (AP: 0.00,
135 mm, ML: ±2.80 mm, DV: -4.85 mm from the Bregma) [44, 45] of CRF-Cre;tdTomato rats
136 (Fig. 3A-3E). Additionally, AAV-DIO-Chrimson-tdTomato was infused into the CeA (AP: -
137 2.60 mm; ML: ±4.20 mm; DV: -8.10 mm) and BNST (AP: -0.10 mm; ML: ±1.40 mm; DV: -
138 6.70 mm) as described in published literature [46] (Fig. 3F-3H). The animals were placed
139 on a stereotaxic surgical frame after being sedated with 3-4% isoflurane at a rate of 1.0
140 L/min, as described previously [41, 42, 47]. These coordinates were obtained from
141 previous publications and verified using the rat [48] or mouse [49] brain atlases. A volume
142 of 0.5 μL/site (mice) or 1 μL/site (rats) of virus was infused at a rate of 0.08 μL/min. At the
143 end of the infusion, the injectors remained at the injection site for 10 to 15 min before
144 removal to allow for virus diffusion. The scalp incision was then sutured and animals were
145 returned to their home cage for recovery.

146 **Histology and cell counting**

147 Animals were anesthetized and perfused intracardially with 4% paraformaldehyde
148 (PFA) in phosphate-buffered saline (PBS). The brains were then extracted and
149 submerged in 4% PFA/PBS solution for one day at 4°C, then transferred to a 30% sucrose
150 solution in PBS. Once the brains completely sank in the sucrose solution, they were cut
151 into 50-μm thick coronal sections using a cryostat. The slices were stored in a PBS bath
152 at 4°C before mounting on slides for imaging using a confocal laser-scanning microscope
153 (Fluoview, Olympus). All images were processed using Imaris 8.3.1 (Bitplane, Zurich,
154 Switzerland) as previously reported [30, 32, 34]. Immunostaining for choline
155 acetyltransferase (ChAT) was performed using an anti-ChAT primary antibody (AB144P),

156 followed by a fluorophore-conjugated secondary antibody (A21447) emitting at 647 nm,
157 labeling CINs with far-red fluorescence. Cell counting was performed in 8 CRF-
158 Cre;tdTomato rats. For each brain region, 5-10 brain sections were imaged from each
159 animal. Imaris was used to quantify green and red neurons as well as evaluate
160 colocalization. Brain regions were identified using the Mouse Brain Atlas [49].

161 **Slice electrophysiology**

162 ***Slice preparation.*** Slices were prepared and electrophysiological recordings were
163 conducted as described previously [30, 32, 41, 42, 50]. Briefly, coronal sections (250 μm)
164 containing the striatum were cut in an ice-cold cutting solution containing (in mM): 40
165 NaCl, 148.5 sucrose, 4 KCl, 1.25 NaH_2PO_4, 25 $NaHCO_3$, 0.5 $CaCl_2$, 7 $MgCl_2$, 10 glucose,
166 1 sodium ascorbate, 3 sodium pyruvate, and 3 myo-inositol. The solution was saturated
167 with 95% O_2 and 5% CO_2. Slices were then incubated in a 1:1 mixture of the cutting and
168 external solutions at 32°C for 45 min. The external solution was composed of the following
169 (in mM): 125 NaCl, 4.5 KCl, 2.5 $CaCl_2$, 1.3 $MgCl_2$, 1.25 NaH_2PO_4, 25 $NaHCO_3$, 15 glucose,
170 and 15 sucrose. The external solution was saturated with 95% O_2 and 5% CO_2. Slices
171 were then maintained in the external solution at room temperature until use.

172 ***Cell-attached recordings.*** Individual slices were transferred to a recording chamber and
173 continuously perfused with the external solution at 2-3 mL/min at 32°C. Fluorescent
174 axonal fibers and neurons were visualized using an epifluorescent microscope (Olympus).
175 The presence of tdTomato and GFP allowed cell type verification and expression of Ai32
176 allowed visualization of CRF-producing fibers. CINs in slices were identified by their
177 labeled color, large size, and spontaneous firing. Spontaneous cell-attached CIN firing
178 activity was recorded for 5 min to calculate the average firing frequency. 470-nm or 590-

nm light was emitted from the objective lens for 2 ms at a frequency and duration specified in the respective figure legend to stimulate axonal fibers containing channelrhodopsin in the dorsal striatum. We used a potassium-based intracellular solution containing (in mM): 123 potassium gluconate, 10 HEPES, 0.2 EGTA, 8 NaCl, 2 MgATP, and 0.3 NaGTP, with an osmolarity of ~280 mOsm/L and the pH adjusted to 7.3 using KOH. For protocols involving alcohol application, we pretreated dorsal striatal slices with alcohol (50 mM) for 1 h outside of the recording chamber. After pretreatment, slices were transferred to the recording chamber, where alcohol was washed out for at least 15 min before recording. The recordings included a 10-min baseline period (without alcohol), followed by 10 min of CRF bath application, and then 10 min of alcohol exposure. Control slices did not receive alcohol pretreatment but were exposed to acute alcohol following CRF application. In both conditions, the final 10-min alcohol application allowed us to assess whether alcohol pretreatment altered the CIN firing response to subsequent CRF and alcohol exposure. In protocols that required inhibition of glutamatergic and $GABA_A$ receptors, DNQX and bicuculline were used, respectively. Electrophysiology data were acquired using Clampex-10 (Molecular Devices) and analyzed using Clampfit-10 (Molecular Devices) and Mini Analysis (Mini60, Synaptosoft Inc.).

Ex vivo live-tissue confocal imaging of ACh release

Brain slices were kept in a recording chamber perfused with external solution flowing and saturated with 95% O_2 and 5% CO_2. An Olympus FluoView FV3000 microscope was used with a 10x NA 0.3 and a 40x NA 0.8 water immersion objective, along with a 488 nm and a 561 nm laser. The sample rate of imaging was 2-3 frames per

201 second. Parameters were maintained consistently across all imaging sessions, including
202 laser intensity, HV, gain, offset, and aperture diameter.

203 **Statistical analysis**

204 Before conducting all experiments shown in this study, we performed a power
205 analysis with SigmaPlot software (12.5, Systat) using the mean and standard deviation
206 from previous studies in our lab [34, 43-45] to determine the required sample sizes to
207 detect a significant difference. We tested all data for normality before significance testing.
208 If the normality test failed, we used nonparametric tests, such as the Mann-Whitney U
209 Test. All data are expressed as the mean ± the standard error of the mean. Data were
210 analyzed by two-tailed *t*-test (unpaired or paired), one- or two-way ANOVA with repeated
211 measurement, followed by the Student-Newman-Keuls (SNK) post hoc test. Significance
212 was determined if $p < 0.05$. Statistical analysis was conducted by the SigmaPlot program.
213 Graphs were constructed using the OriginPro (2024b, OriginLab) program.

214

Results

Dorsal Striatal CINs Receive Monosynaptic Inputs From CeA and BNST Neurons

To investigate the connection between dorsal striatal CINs and stress-related brain regions, we examined whether CINs receive monosynaptic inputs from the CeA and the BNST [51, 52]. We used ChAT-Cre;D1-tdTomato mice to perform rabies-mediated monosynaptic retrograde tracing. In this mouse model, CINs express Cre recombinase and dopamine D1-receptor (D1R)-expressing medium spiny neurons (D1-MSNs) are labeled with tdTomato. Including the D1-tdTomato marker allowed us to delineate the CeA and BNST, which do not express D1Rs unlike surrounding striatal areas [47]. We performed rabies-mediated retrograde monosynaptic circuit tracing (Fig. 1A), allowing specific targeting of CINs (Fig. 1B). In addition to labeling neurons in brain regions known to project to dorsal striatal CINs, we were surprised to see labeled neurons in both the CeA (Fig. 1C) and BNST (Fig. 1D), which are well-characterized as key stress-responsive nuclei. Interestingly, we observed significantly more GFP^+ neurons in the BNST than in the CeA (Fig. 1E; Mann-Whitney U = 29.500, ***$p < 0.001$). These results demonstrate that dorsal striatal CINs receive direct, monosynaptic inputs from neurons in the CeA and BNST. Together, these findings highlight the anatomical connection of dorsal striatal CINs with key stress-responsive brain regions.

The Dorsal Striatum Lacks CRF^+ Neurons Unlike the CeA and BNST

We first investigated whether the dorsal striatum contains CRF producing cells or if CRF signaling in the dorsal striatum instead depends on CeA and BNST inputs. While previous studies have identified CRF-producing neurons in the CeA and BNST [46], their

presence in the dorsal striatum remains uncertain. Coronal brain sections from CRF-Cre;tdTomato rats revealed dense populations of CRF-tdTomato$^+$ neurons in the CeA (Fig. 2A) and BNST (Fig. 2B). Although CRF$^+$ axonal fibers were observed in the dorsal striatum, CRF$^+$ cell bodies were largely absent (Fig. 2C). Quantitative analysis confirmed significant regional differences, indicating that the CeA and BNST contained substantially more CRF$^+$ neurons than the dorsal striatum (Fig. 2D; CeA versus DS, Q = 7.30, $*p < 0.05$; BNST versus DS, Q = 3.72, $*p < 0.05$). Notably, the CeA exhibited a higher number of CRF$^+$ neurons compared with the BNST (Fig. 2D; Q = 2.75, $*p < 0.05$). The apparent lack of CRF$^+$ cell bodies in the dorsal striatum suggests that CRF signaling in the dorsal striatum arises from CRF$^+$ neurons in the CeA and BNST.

Dorsal Striatum CINs Receive Monosynaptic CRF$^+$ Inputs from the CeA and BNST

To test whether CRF$^+$ neurons in the CeA and BNST project to the dorsal striatum, we infused a retrograde adeno-associated virus into the dorsal striatum of CRF-Cre;tdTomato rats. This strategy allows CRF$^+$ neurons (tdTomato$^+$) that project to the dorsal striatum to also be labeled with GFP (Fig. 3A). Confocal imaging revealed GFP$^+$ neurons in both the BNST (Fig. 3B) and CeA (Fig. 3C), with many overlapping GFP-labeled dorsal striatum-projecting neurons and tdTomato-positive (CRF$^+$) cells in both regions. This indicates that CRF$^+$ neurons from the CeA and BNST project to the dorsal striatum. Despite the CeA containing more CRF$^+$ neurons than the BNST, as we observed above, the proportion of dorsal striatum-projecting CRF$^+$ neurons was higher in the BNST than in the CeA (Fig. 3D, 3E; $t_{15} = 5.49$, $***p < 0.001$; $t_{15} = -5.01$, $***p < 0.001$). However, the total number of dorsal striatum-projecting CRF$^+$ neurons did not differ between the

CeA and BNST (Fig. 3F; $t_{15} = -0.78$, $p > 0.05$). These results indicate that CRF^+ neurons in the CeA and BNST project to the dorsal striatum.

To test whether CRF neurons in the CeA and BNST make monosynaptic projections to dorsal striatal CINs, we performed ChR2-assisted circuit tracing. Given that both the CeA and BNST are primarily GABAergic nuclei [53, 54], we examined whether optogenetic stimulation of CRF-containing projections to the dorsal striatum induce inhibitory monosynaptic currents in CINs. To test this, we infused AAV-FLEX-Chrimson-tdTomato into the CeA and BNST of CRF-Cre;ChAT-eGFP mice so that we could selectively stimulate CRF-containing fibers in the dorsal striatum while recording from GFP labeled CINs (Fig. 3G). We found that optogenetic stimulation of CRF^+ fibers with yellow light evoked fast synaptic currents in dorsal striatal CINs (Fig. 3H). This response was abolished by TTX (Fig. 3H, 3I; BL versus TTX: $q = 4.16$, $^*p < 0.05$) but restored using TTX+4-AP (Fig. 3H, 3I; TTX vs TTX+4-AP: $q = 4.73$, $^*p < 0.05$), suggesting the existence of monosynaptic transmission. Notably, the restored synaptic response was predominantly blocked by the $GABA_A$ receptor antagonist bicuculline (Fig. 3H, 3I; TTX+4-AP versus TTX+4-AP+Bic: $q = 4.44$, $^*p < 0.05$), demonstrating that evoked currents are GABAergic. Together, these results demonstrate that dorsal striatal CINs receive monosynaptic GABAergic synapses from the CRF^+ neurons in the CeA and BNST, suggesting that CRF^+ neurons project to the dorsal striatum and release CRF to modulate cholinergic signaling in the dorsal striatum.

Striatal CINs Express CRFR1

Having established that CINs receive monosynaptic inputs from CRF neurons in the CeA and BNST, we next replicated the finding that CINs express the CRF receptor, CRFR1 [15, 55, 56]. To address this, we used CRFR1-Cre-tdTomato rats [28], in which CRFR1-containing neurons express Cre recombinase and are visible due to the tdTomato label. Confocal imaging of striatal sections from these rats confirmed that CRFR1-expressing neurons are distributed throughout the striatum (Fig. 4A). To verify that CRFR1-positive ($CRFR1^+$) neurons are also cholinergic, we stained sections with an anti-ChAT antibody and imaged them using confocal microscopy (Fig. 4A). We found that ~30% of CINs express CRFR1 (Fig. 4B, 4C; Mann-Whitney U = 0.000, ***$p < 0.001$). These findings align with previous reports that a subset of striatal CINs express CRFR1, suggesting that the striatum is involved in CRFR1-mediated signaling pathways.

CRF Enhances CIN Activity and Acetylcholine Release in the Dorsal Striatum

Following the finding that CRF^+ neurons send inputs to the dorsal striatum, we sought to investigate how CRF might influence CIN spontaneous firing activity. Cell-attached electrophysiology recordings of GFP^+ neurons in the dorsal striatum were performed in ChAT-eGFP mice before and during bath application of CRF (100 nM) (Fig. 5A). We found that CRF significantly increased CIN firing frequency above baseline (Fig. 5B, 5C; $t_{(8)} = -24.08$, ***$p < 0.001$). This effect was abolished by pre-treatment with the CRFR1 antagonist NBI 35695 (Fig. 5C; Mann-Whitney U = 0.000, ***$p < 0.001$), confirming that CRF potentiates CIN firing via CRFR1 activation in the dorsal striatum.

Because CINs are the primary source of ACh in the dorsal striatum, we next examined whether CRF-induced CIN activation enhances ACh release. To do so, we

infused an adeno-associated virus (AAV) introducing a genetically encoded ACh sensor (AAV-GRAB$_{ACh4m}$) into the dorsal striatum of wildtype mice [40]. Live-tissue confocal imaging was performed on brain slices containing the dorsal striatum 14 days post-infusion to monitor ACh levels (Fig. 5D). Bath application of CRF produced a robust ACh fluorescence signal (Fig. 5E, 5F; Mann-Whitney U = 7.000, $*p < 0.05$), indicating that CRF enhances the release of ACh. These results suggest that CRF-driven CIN activation increases ACh release in the dorsal striatum.

To further determine whether direct activation of CRF-expressing fibers modulates CIN activity, we used an optogenetic approach. We generated CRF-Cre;Ai32;ChAT-eGFP mice to selectively stimulate CRF$^+$ terminals in the dorsal striatum. Cell-attached electrophysiology recordings were conducted in CINs while blue light (470 nm, 50 Hz, 60 s) was used to activate local ChR2-expressing CRF$^+$ fibers (Fig. 5G). Burst stimulation of CRF$^+$ terminals significantly and reversibly increased CIN firing in the presence of DNQX and bicuculline (Fig. 5H, 5I; Pre versus Stim, q = 3.69, $*p < 0.05$; Stim versus Post, q = 11.82, $***p < 0.001$). Together, these findings demonstrate that CRF enhances CIN activity and ACh release in the dorsal striatum.

Acute Alcohol Application Attenuates CRF-Mediated Enhancement of CIN Firing

Given that acute alcohol exposure suppresses CIN activity [20], we next examined the impact of alcohol on CRF-mediated enhancement of CIN firing. We first assessed how alcohol alone influences CIN firing by measuring spontaneous CIN activity before, during, and after bath application of 50 mM alcohol in dorsal striatal slices from ChAT-eGFP mice. Consistent with previous reports [20], acute alcohol suppressed CIN

spontaneous firing in cell-attached recordings, an effect that was reversed after a washout period (Fig. 6A, 6B; Mann-Whitney U = 0.000, *$p < 0.05$).

To determine how acute alcohol exposure affects CRF-induced enhancement of CIN firing, we pretreated dorsal striatal slices with alcohol (50 mM) for 1 h outside of the recording chamber (Fig. 6C). In control slices, CRF significantly increased the spontaneous firing of dorsal striatal CINs, consistent with our previous findings (Fig. 6D; BL versus CRF, q = 11.51, ***$p < 0.001$; see also Fig. 5B). Subsequent alcohol application reduced firing but maintained a level still higher than the baseline (Fig. 6D; CRF versus EtOH, q = 6.21, **$p < 0.01$; BL versus EtOH, q = 5.29, **$p < 0.01$). This residual increase is likely due to the persistent effect of exogenous CRF, which is sustained for several minutes (Fig. 5B).

In slices pretreated with alcohol, CRF still increased CIN firing frequency, but subsequent alcohol application failed to suppress it back to baseline (Fig. 6E; BL versus CRF, q = 5.20, **$p < 0.01$; CRF versus EtOH, q = 6.21, $p = 0.05$). This suggests that prior acute alcohol exposure reduces the ability of subsequent alcohol exposure to suppress CIN activity in the presence of CRF. Notably, when comparing the change in CIN firing from baseline to CRF application, alcohol pretreatment significantly blunted CRF-induced enhancement of CIN firing (Fig. 6F; $t_{18} = 2.70$, *$p < 0.05$). Together, these findings demonstrate that acute alcohol attenuates subsequent CRF-mediated enhancement of CIN firing, suggesting a potential mechanism by which alcohol and CRF interact to modulate striatal cholinergic activity.

Discussion

This study identifies a circuit in which CRF-positive neurons in the CeA and BNST provide direct input to dorsal striatal CINs that express CRFR1. CRF enhances CIN excitability and ACh release, linking CRF to cholinergic modulation. In addition, alcohol exposure and withdrawal blunt this effect, suggesting a possible role for CRF signaling to dorsal striatal CINs in the etiology of alcohol use disorder. Using monosynaptic and retrograde circuit tracing, we identified direct projections from CRF-expressing neurons in the CeA and BNST to dorsal striatal CINs. Functional electrophysiology shows that CRF enhances CIN excitability and promotes ACh release via CRFR1 receptors. However, acute alcohol exposure and withdrawal disrupted this excitatory effect, indicating that alcohol interferes with CRF-dependent cholinergic modulation. These findings identify a CRF–CIN circuit that is vulnerable to alcohol-induced dysregulation, providing mechanistic insight into how CRF and alcohol interact to impair striatal function. Our results highlight CRF signaling in the dorsal striatum as a potential therapeutic target for mitigating the cognitive flexibility deficits and reward system dysfunction seen in AUD.

Monosynaptic Inputs from the CeA and BNST to CINs

Tracing experiments reported here show that dorsal striatal CINs receive direct synaptic input from CRF-expressing neurons in the CeA and BNST, regions involved in stress and emotion [53, 57]. While previous studies have identified CeA and BNST projections to the striatum, they did not show that they arise from CRF neurons or that they target CINs [47, 58-60]. Our results establish a direct CRF-to-CIN pathway, linking CRF release to cholinergic modulation. Given CINs' roles in striatal output, behavioral

flexibility, and reward learning [45, 61-64], this circuit likely contributes to stress-driven behavioral adaptations [53, 65-68].

We found that there are no CRF neurons in the dorsal striatum, indicating that CRF signaling in the dorsal striatum arises from inputs outside of the striatum, including from the CeA and BNST. Electrophysiological experiments show that CRF fiber stimulation enhances CIN excitability in the presence of synaptic blockers, supporting a role for CRF signaling in the modulation of striatal cholinergic tone. The transient effects of endogenous CRF release, compared to prolonged effects of CRF bath application, suggest that CRF signaling in the striatum may generate dynamic patterns of cholinergic activation to influence behavioral expression.

Alcohol Disrupts CRF-Mediated CIN Excitation

A key finding of this study is that alcohol exposure disrupts CRF-mediated CIN excitation. Both acute alcohol exposure and withdrawal attenuate the CRF-induced increase in CIN activity, indicating that alcohol alters the responsiveness of these neurons to stress signals. Because stress is a well-established trigger for alcohol relapse [69-71], the observed alcohol-induced disruption in CRF signaling may impair the brain's ability to adaptively respond to stress, thereby increasing susceptibility to relapse.

One possibility is that alcohol exposure downregulates CRFR1 expression [72, 73] or alters CIN function [44], reducing their responsiveness to stress-related input [74, 75]. Alternatively, alcohol may interfere with intracellular signaling cascades downstream of CRFR1 activation, leading to diminished excitability and ACh release. The mechanisms underlying alcohol's effect on CRF signaling in CINs remain to be fully elucidated.

Implications for Alcohol Use Disorder

By delineating a CRF-to-CIN pathway linking the extended amygdala to the dorsal striatum, our findings provide critical insights into how stress and alcohol interact at the circuit level to shape behavior. Given the role of CINs in action selection and behavioral flexibility [76], disruption of this stress-sensitive cholinergic circuit may underlie the decision-making deficits and compulsive alcohol-seeking behavior observed in AUD [43-45, 77-79].

In summary, we identify a direct CRF-positive projection from the CeA and BNST to dorsal striatal CINs, revealing a new mechanism by which stress can modulate cholinergic signaling in the striatum. We demonstrate that CRF enhances CIN excitability and ACh release, and that alcohol exposure disrupts this modulation. These findings highlight the CRF–CIN circuit as a potential therapeutic target in AUD and suggest that restoring CRF signaling may help counteract stress- and alcohol-induced striatal dysfunction. Future work should assess whether pharmacological or circuit-based interventions targeting CRFR1 or CINs can mitigate behavioral impairments in individuals with AUD.

Acknowledgements

This research was supported by NIAAA R01AA021505 (JW), R01AA027768 (JW), U01AA025932 (JW), R01MH112768 (NJ), and R21AG086907 (NJ).

The authors declare no competing financial interests.

References

1. Heilig, M. and G.F. Koob, *A key role for corticotropin-releasing factor in alcohol dependence.* Trends in Neurosciences, 2007. 30(8): p. 399-406.
2. Becker, H.C., *Effects of Alcohol Dependence and Withdrawal on Stress Responsiveness and Alcohol Consumption.* Alcohol Research-Current Reviews, 2012. 34(4): p. 448-458.
3. Quadros, I.M.H., et al., *An Update on CRF Mechanisms Underlying Alcohol Use Disorders and Dependence.* Frontiers in Endocrinology, 2016. 7: p. 134.
4. Bruijnzeel, A.W. and M.S. Gold, *The role of corticotropin-releasing factor-like peptides in cannabis, nicotine, and alcohol dependence.* Brain Research Reviews, 2005. 49(3): p. 505-528.
5. Roberto, M., et al., *Corticotropin-Releasing Factor (CRF) and Addictive Behaviors.* International Review of Neurobiology, 2017. 136: p. 5-51.
6. Koob, G.F., *Stress, corticotropin-releasing factor, and drug addiction.* Ann N Y Acad Sci, 1999. 897: p. 27-45.
7. Haass-Koffler, C.L. and S.E. Bartlett, *Stress and addiction: contribution of the corticotropin releasing factor (CRF) system in neuroplasticity.* Front Mol Neurosci, 2012. 5: p. 91.

8. Koob, G.F., *A role for brain stress systems in addiction.* Neuron, 2008. 59(1): p. 11-34.

9. Shalev, U., S. Erb, and Y. Shaham, *Role of CRF and other neuropeptides in stress-induced reinstatement of drug seeking.* Brain Res, 2010. 1314: p. 15-28.

10. Baumgartner, H.M., J. Schulkin, and K.C. Berridge, *Activating Corticotropin-Releasing Factor Systems in the Nucleus Accumbens, Amygdala, and Bed Nucleus of Stria Terminalis: Incentive Motivation or Aversive Motivation?* Biological Psychiatry, 2021. 89(12): p. 1162-1175.

11. Kimchi, E.Y., et al., *Neuronal correlates of instrumental learning in the dorsal striatum.* J Neurophysiol, 2009. 102(1): p. 475-89.

12. Nonomura, S., et al., *Monitoring and Updating of Action Selection for Goal-Directed Behavior through the Striatal Direct and Indirect Pathways.* Neuron, 2018. 99(6): p. 1302-1314 e5.

13. Redgrave, P., et al., *Goal-directed and habitual control in the basal ganglia: implications for Parkinson's disease.* Nat Rev Neurosci, 2010. 11(11): p. 760-72.

14. Mantsch, J.R., *Corticotropin releasing factor and drug seeking in substance use disorders: Preclinical evidence and translational limitations.* Addict Neurosci, 2022. 4.

15. Lemos, J.C., J.H. Shin, and V.A. Alvarez, *Striatal cholinergic interneurons are a novel target of corticotropin releasing factor.* Journal of Neuroscience, 2019: p. 5647-5661.

16. Carboni, L., et al., *Increased expression of CRF and CRF-receptors in dorsal striatum, hippocampus, and prefrontal cortex after the development of nicotine sensitization in rats.* Drug Alcohol Depend, 2018. 189: p. 12-20.

17. Abudukeyoumu, N., et al., *Cholinergic modulation of striatal microcircuits.* European Journal of Neuroscience, 2019. 49(5): p. 604-622.

18. Tanimura, A., et al., *Striatal cholinergic interneurons and Parkinson's disease.* European Journal of Neuroscience, 2018. 47(10): p. 1148-1158.

19. Chantranupong, L., et al., *Dopamine and glutamate regulate striatal acetylcholine in decision-making.* Nature, 2023. 621(7979): p. 577.

20. Blomeley, C.P., et al., *Ethanol affects striatal interneurons directly and projection neurons through a reduction in cholinergic tone.* Neuropsychopharmacology, 2011. 36(5): p. 1033-46.

21. Lim, S.A., U.J. Kang, and D.S. McGehee, *Striatal cholinergic interneuron regulation and circuit effects.* Front Synaptic Neurosci, 2014. 6: p. 22.

22. Li, J., et al., *The Orbitofrontal Cortex to Striatal Cholinergic Interneuron Circuit Controls Cognitive Flexibility Shaping Alcohol-Seeking Behavior.* Biological Psychiatry, 2025. 97(6): p. 614-626.

23. Tallini, Y.N., et al., *BAC transgenic mice express enhanced green fluorescent protein in central and peripheral cholinergic neurons.* Physiological Genomics, 2006. 27(3): p. 391-7.

24. Rossi, J., et al., *Melanocortin-4 receptors expressed by cholinergic neurons regulate energy balance and glucose homeostasis.* Cell Metabolism, 2011. 13(2): p. 195-204.

25. Ade, K.K., et al., *An Improved BAC Transgenic Fluorescent Reporter Line for Sensitive and Specific Identification of Striatonigral Medium Spiny Neurons.* Frontiers in Systems Neuroscience, 2011. 5: p. 32.

26. Madisen, L., et al., *A toolbox of Cre-dependent optogenetic transgenic mice for light-induced activation and silencing.* Nature Neuroscience, 2012. 15(5): p. 793-802.

27. Taniguchi, H., et al., *A resource of Cre driver lines for genetic targeting of GABAergic neurons in cerebral cortex.* Neuron, 2011. 71(6): p. 995-1013.

28. Weera, M.M., et al., *Generation of a CRF-Cre transgenic rat and the role of central amygdala CRF cells in nociception and anxiety-like behavior.* Elife, 2022. 11.

29. Pomrenze, M.B., et al., *A Transgenic Rat for Investigating the Anatomy and Function of Corticotrophin Releasing Factor Circuits.* Frontiers in Neuroscience, 2015. 9: p. 487.

30. Lu, J., et al., *Alcohol intake enhances glutamatergic transmission from D2 receptor-expressing afferents onto D1 receptor-expressing medium spiny neurons in the dorsomedial striatum.* Neuropsychopharmacology, 2019. 44(6): p. 1123-1131.

31. Wang, J., et al., *Alcohol Elicits Functional and Structural Plasticity Selectively in Dopamine D1 Receptor-Expressing Neurons of the Dorsomedial Striatum.* Journal of Neuroscience, 2015. 35(33): p. 11634-43.

32. Cheng, Y., et al., *Distinct Synaptic Strengthening of the Striatal Direct and Indirect Pathways Drives Alcohol Consumption.* Biological Psychiatry, 2017. 81(11): p. 918-929.

33. Cheng, Y., et al., *Prenatal Exposure to Alcohol Induces Functional and Structural Plasticity in Dopamine D1 Receptor-Expressing Neurons of the Dorsomedial Striatum.* Alcoholism: Clinical and Experimental Research, 2018.

34. Wei, X., et al., *Dopamine D1 or D2 receptor-expressing neurons in the central nervous system.* Addiction Biology, 2018. 23(2): p. 569-584.

35. Watabe-Uchida, M., et al., *Whole-brain mapping of direct inputs to midbrain dopamine neurons.* Neuron, 2012. 74(5): p. 858-73.

36. Klapoetke, N.C., et al., *Independent optical excitation of distinct neural populations.* Nat Methods, 2014. 11(3): p. 338-46.

37. Oh, S.W., et al., *A mesoscale connectome of the mouse brain.* Nature, 2014. 508(7495): p. 207-14.

38. Wickersham, I.R., et al., *Monosynaptic restriction of transsynaptic tracing from single, genetically targeted neurons.* Neuron, 2007. 53(5): p. 639-47.

39. Wang, L., et al., *Characteristics of GABAergic and cholinergic neurons in perinuclear zone of mouse supraoptic nucleus.* J Neurophysiol, 2015. 113(3): p. 754-67.

40. Jing, M., et al., *An optimized acetylcholine sensor for monitoring in vivo cholinergic activity.* Nat Methods, 2020. 17(11): p. 1139-1146.

41. Ma, T., et al., *Bidirectional and long-lasting control of alcohol-seeking behavior by corticostriatal LTP and LTD.* Nature Neuroscience, 2018. 21(3): p. 373-383.

42. Hellard, E.R., et al., *Optogenetic control of alcohol-seeking behavior via the dorsomedial striatal circuit.* Neuropharmacology, 2019. 155: p. 89-97.

43. Gangal, H., et al., *Drug reinforcement impairs cognitive flexibility by inhibiting striatal cholinergic neurons.* Nature Communications, 2023. 14(1): p. 3886.

44. Ma, T., et al., *Chronic alcohol drinking persistently suppresses thalamostriatal excitation of cholinergic neurons to impair cognitive flexibility.* Journal of Clinical Investigation, 2022. 132(4): p. e154969.

45. Huang, Z., et al., *Dynamic responses of striatal cholinergic interneurons control behavioral flexibility.* Science Advances, 2024. 10(51): p. eadn2446.

46. de Guglielmo, G., et al., *Inactivation of a CRF-dependent amygdalofugal pathway reverses addiction-like behaviors in alcohol-dependent rats.* Nature Communications, 2019. 10(1): p. 1238.

47. Lu, J.Y., et al., *Whole-Brain Mapping of Direct Inputs to Dopamine D1 and D2 Receptor-Expressing Medium Spiny Neurons in the Posterior Dorsomedial Striatum.* Eneuro, 2021. 8(1).

48. Paxinos, G., C.R. Watson, and P.C. Emson, *AChE-stained horizontal sections of the rat brain in stereotaxic coordinates.* Journal of Neuroscience Methods, 1980. 3(2): p. 129-49.

49. Franklin, K.B.J. and G. Paxinos, *The mouse brain in stereotaxic coordinates*. 3 ed. 2007, San Diego: Academic Press.

50. Ma, T., et al., *Alcohol induces input-specific aberrant synaptic plasticity in the rat dorsomedial striatum.* Neuropharmacology, 2017. 123: p. 46-54.

51. Davis, M., *Neural systems involved in fear and anxiety measured with fear-potentiated startle.* American Psychologist, 2006. 61(8): p. 741-756.

52. Funk, C.K., et al., *Corticotropin-releasing factor within the central nucleus of the amygdala mediates enhanced ethanol self-administration in withdrawn, ethanol-dependent rats.* Journal of Neuroscience, 2006. 26(44): p. 11324-11332.

53. Partridge, J.G., et al., *Stress increases GABAergic neurotransmission in CRF neurons of the central amygdala and bed nucleus stria terminalis.* Neuropharmacology, 2016. 107: p. 239-250.

54. Sanford, C.A., et al., *A Central Amygdala CRF Circuit Facilitates Learning about Weak Threats.* Neuron, 2017. 93(1): p. 164-178.

55. Chen, A., *Genetic Dissection of the Neuroendocrine and Behavioral Responses to Stressful Challenges*, in *Stem Cells in Neuroendocrinology*, D. Pfaff and Y. Christen, Editors. 2016: Cham (CH). p. 69-79.

56. Olson, K.L., et al., *Cholinergic interneurons in the nucleus accumbens are a site of cellular convergence for corticotropin-releasing factor and estrogen regulation in male and female mice.* European Journal of Neuroscience, 2024. 60(5): p. 4937-4953.

57. Kim, S.Y., et al., *Diverging neural pathways assemble a behavioural state from separable features in anxiety.* Nature, 2013. 496(7444): p. 219-23.

58. Giovanniello, J.R., et al., *A dual-pathway architecture for stress to disrupt agency and promote habit.* Nature, 2025.

59. Smith, J.B., et al., *Genetic-Based Dissection Unveils the Inputs and Outputs of Striatal Patch and Matrix Compartments.* Neuron, 2016. 91(5): p. 1069-1084.

60. Heaton, E.C., et al., *Control of goal-directed and inflexible actions by dorsal striatal melanocortin systems, in coordination with the central nucleus of the amygdala.* Progress in Neurobiology, 2024. 238: p. 102629.

61. Duhne, M., et al., *A mismatch between striatal cholinergic pauses and dopaminergic reward prediction errors.* Proceedings of the National Academy of Sciences of the United States of America, 2024. 121(41): p. e2410828121.

62. Ostlund, S.B., et al., *Modulation of cue-triggered reward seeking by cholinergic signaling in the dorsomedial striatum.* European Journal of Neuroscience, 2017. 45(3): p. 358-364.

63. Dautan, D., et al., *Cholinergic midbrain afferents modulate striatal circuits and shape encoding of action strategies.* Nature Communications, 2020. 11(1): p. 1739.

64. Aoki, S., et al., *Cholinergic interneurons in the rat striatum modulate substitution of habits.* European Journal of Neuroscience, 2018. 47(10): p. 1194-1205.

65. Rieger, N.S., et al., *Insular cortex corticotropin-releasing factor integrates stress signaling with social affective behavior.* Neuropsychopharmacology, 2022. 47(6): p. 1156-1168.

66. Alizamini, M.M., et al., *Corticotropin-releasing factor receptor 1 in infralimbic cortex modulates social stress-altered decision-making.* Progress in Neuro-Psychopharmacology & Biological Psychiatry, 2022. 116: p. 110523.

67. Bryce, C.A. and S.B. Floresco, *Perturbations in Effort-Related Decision-Making Driven by Acute Stress and Corticotropin-Releasing Factor.* Neuropsychopharmacology, 2016. 41(8): p. 2147-59.

68. Pomrenze, M.B., et al., *A Corticotropin Releasing Factor Network in the Extended Amygdala for Anxiety.* Journal of Neuroscience, 2019. 39(6): p. 1030-1043.

69. Bertotto, M.E., et al., *Increased voluntary ethanol consumption and c-Fos expression in selected brain areas induced by fear memory retrieval in ethanol withdrawn rats.* European Neuropsychopharmacology, 2010. 20(8): p. 568-81.

70. Becker, H.C., et al., *Oxytocin Reduces Sensitized Stress-Induced Alcohol Relapse in a Model of Posttraumatic Stress Disorder and Alcohol Use Disorder Comorbidity.* Biological Psychiatry, 2023. 94(3): p. 215-225.

71. Walker, L.C., H.E. Kastman, and A.J. Lawrence, *Pattern of neural activation following yohimbine-induced reinstatement of alcohol seeking in rats.* European Journal of Neuroscience, 2020. 51(3): p. 706-720.

72. Hansson, A.C., et al., *Region-specific down-regulation of gene expression in alcohol-preferring msP rats following access to alcohol.* Addiction Biology, 2007. 12(1): p. 30-34.

73. Zhou, Y., et al., *Reduced hypothalamic POMC and anterior pituitary CRF1 receptor mRNA levels after acute, but not chronic, daily "binge" intragastric alcohol administration.* Alcoholism: Clinical and Experimental Research, 2000. 24(10): p. 1575-82.

74. Besheer, J., et al., *Stress hormone exposure reduces mGluR5 expression in the nucleus accumbens: functional implications for interoceptive sensitivity to alcohol.* Neuropsychopharmacology, 2014. 39(10): p. 2376-86.

75. Sayette, M.A., et al., *A test of the appraisal-disruption model of alcohol and stress.* Journal of Studies on Alcohol, 2001. 62(2): p. 247-256.

76. Bradfield, L.A., et al., *The thalamostriatal pathway and cholinergic control of goal-directed action: interlacing new with existing learning in the striatum.* Neuron, 2013. 79(1): p. 153-66.

77. Zorrilla, E.P., M.L. Logrip, and G.F. Koob, *Corticotropin releasing factor: a key role in the neurobiology of addiction.* Frontiers in Neuroendocrinology, 2014. 35(2): p. 234-44.

78. Moberg, C.A., et al., *Increased startle potentiation to unpredictable stressors in alcohol dependence: Possible stress neuroadaptation in humans.* Journal of Abnormal Psychology, 2017. 126(4): p. 441-453.

79. Koob, G.F. and L. Vendruscolo, *Theoretical Frameworks and Mechanistic Aspects of Alcohol Addiction: Alcohol Addiction as a Reward Deficit/Stress Surfeit Disorder.* Current Topics in Behavioral Neurosciences, 2023.

Figure Legends

Figure 1. Dorsal Striatal CINs Receive Monosynaptic Inputs From the CeA and BNST

A, Schematic illustrating the infusion of helper viruses (AAV-DIO-TVA-mCherry and AAV-DIO-RG) and rabies-GFP (RV-GFP) into the dorsal striatum of ChAT-Cre;D1-tdTomato mice. The rabies-GFP was infused 3 weeks after the helper virus infusion, and animals were euthanized one week after the rabies infusion. **B,** Model for the retrograde transsynaptic labeling of CeA and BNST neurons projecting to dorsal striatal CINs. TVA permits selective infection by the rabies-GFP virus, while RG mediates the retrograde transsynaptic jump from postsynaptic CINs to presynaptic terminals of CeA or BNST neurons. **C,** Sample image showing CeA neurons projecting to dorsal striatal CINs, as indicated by rabies-GFP expression. AP: -1.50 mm from Bregma. TS, tail of the striatum. Scale bar: 0.5 mm, 50 μm for insert. **D,** Sample image demonstrating that BNST neurons project to dorsal striatal CINs, as indicated by rabies-GFP expression. Note that the injection site (inj. site) is also displayed in the dorsal striatum. AP: -0.26 mm from Bregma. DS, dorsal striatum; ac, anterior commissure. Scale bar: 0.5 mm, 50 μm for insert. **E,** The CeA and BNST both send projections to the dorsal striatum, with the BNST providing more inputs. ***$p < 0.001$ by Mann-Whitney test. n = 13 sections from 4 mice (13/4) for the CeA and 18/4 for the BNST.

Figure 2. CRF-Positive Neurons Are Abundant in the CeA and BNST but Absent in the Dorsal Striatum

A, **B,** Confocal images showing dense populations of tdTomato-labeled CRF^+ neurons in the CeA (A) and BNST (B) of CRF-Cre;tdTomato rats. AP: -1.5 mm from Bregma (A) and -0.26 mm (B). Scale bars: 1 mm (left) and 50 µm (right). DS, dorsal striatum. **C**, Representative image of the dorsal striatum showing the presence of CRF^+ axonal fibers but the absence of CRF^+ cell bodies. AP: -0.26 mm from Bregma. Scale bar: 100 µm. **D**, The CeA and BNST contain more CRF^+ neurons than the dorsal striatum. $*p < 0.05$ by Kruskal-Wallis with Dunn's Method. n = 20 slices from 7 rats (20/7) for the CeA, 29/7 for the striatum, and 15/7 for the BNST.

Figure 3. CINs Receive Monosynaptic Input From CeA and BNST CRF^+ Neurons

A, Schematic showing virus injection (AAVretro-DIO-GFP) into the dorsal striatum of CRF-Cre;tdTomato rats. **B,** Representative image showing the injection site of AAVretro-DIO-GFP in the posterior dorsal striatum of CRF-Cre;tdTomato rats. Overlapping $tdTomato^+$ (CRF^+) and dorsal striatum-derived Cre-driven GFP^+ expression in the BNST (depicted in yellow) indicates that these CRF^+ neurons project to the dorsal striatum. ac**,** anterior commissure; LV**,** left ventricle; tdT**,** tdTomato; DS-proj, dorsal-striatum-projecting. Scale bar: 0.5 mm (left), 10 µm (right). **C,** Images showing the overlap (in yellow) of $tdTomato^+$ (CRF^+) and dorsal striatum-derived Cre-driven GFP^+ expression in the CeA, confirming that these CRF^+ neurons also project to the dorsal striatum. TS**,** the tail of the striatum. Scale bar: 1 mm (left), 10 µm (right). **D,** The CeA contains more CRF^+ neurons than the BNST. $***p < 0.001$ by unpaired t test, n = 9 sections from 5 rats (9/5) for the

CeA and 8/5 for the BNST. **E,** The proportion of CRF^+ neurons projecting to the dorsal striatum is higher in the BNST compared to the CeA. ***$p < 0.001$ by unpaired t test, n = 9/5 (CeA) and 8/5 (BNST). **F,** The total number of dorsal striatum-projecting CRF^+ neurons does not differ between these two regions. n.s., not significant, $p > 0.05$. n = 9/5 (CeA) and 8/5 (BNST). **G,** Schematic showing the injection of AAV-FLEX-Chrimson-tdTomato into the CeA and BNST of CRF-Cre;ChAT-eGFP mice and the subsequent recording of green striatal CINs during blue light stimulation of surrounding Chrimson-containing fibers from CRF^+ neurons. Fibers were stimulated at a wavelength of 590 nm for 2 ms. **H,** Sample traces showing CIN responses to blue light stimulation of CRF fibers, which were abolished by TTX, recovered with TTX+4-AP and further eliminated by bicuculline (Bic). **I,** Summary of oIPSC data showing the disappearance of oIPSCs with TTX and reappearance with TTX and 4-AP. *$p < 0.05$ by one-way ANOVA. n = 4 slices.

Figure 4. CRFR1 is Expressed in Striatal CINs

A, Representative image of a coronal striatal section from a CRFR1-Cre-tdTomato rat showing CRFR1 expression overlapping with anti-ChAT immunoreactivity. The section was stained using an anti-ChAT antibody and imaged using a far-red (647 nm) wavelength (white). Scale bars: 1 mm (left), 100 µm (middle), and 20 µm (right). **B,** There are significantly fewer $CRFR1^+$ CINs than the total number of CINs in the dorsal striatum. ***$p < 0.001$ by Mann-Whitney test. n = 8 sections from 2 rats. **C,** Around 30% of CINs express CRFR1. n = 8 sections from 2 rats.

Figure 5. CRF Enhances CIN Activity and ACh Release in the Dorsal Striatum

A, Sample images of GFP-labeled CINs in the striatum of a ChAT-eGFP mouse. Scale bar: 0.5 mm, 50 μm (inset). **B**, Bath application of CRF (100 nM) increased the spontaneous firing of dorsal striatal CINs in cell-attached electrophysiological recordings. This effect was prevented by pretreatment with the CRFR1 antagonist NBI 35695 (5 μM). n = 7 cells from 3 mice (7/3) for CRF and 6/3 for CRF plus antagonist recordings. **C,** Data showing that CRF significantly increases the firing from baseline and the firing frequency in the presence of CRF following pretreatment with CRFR1 antagonist is significantly lower. ***$p < 0.001$ by paired t-test, ***$p < 0.001$ by Mann Whitney test. n = 7 cells from 3 mice. **D,** Sample images of ACh sensor fluorescence in dorsal striatal slices before and during bath application of CRF (100 nM). AAV-$GRAB_{ACh4m}$ was infused into the dorsal striatum of wildtype mice, and live-tissue confocal imaging was conducted two weeks post-infusion. Scale bar: 10 μm for left and right. **E,** Sample trace of spontaneous ACh release events (indicated by red arrows, top). Bath application of CRF increased ACh sensor fluorescence (bottom). **F,** Summary data showing a significant increase in ACh sensor fluorescence following CRF application. *$p < 0.05$ by Mann-Whitney test. n = 7 slices from 7 mice. **G,** Schematic of cell-attached electrophysiological recordings from dorsal striatal CINs in CRF-Cre;Ai32;ChAT-eGFP mice, with simultaneous optogenetic stimulation of CRF^+ fibers using blue light (470-nm, 2 ms, 50 Hz, 60 sec). **H,** Sample trace showing the increase in CIN firing frequency during blue light stimulation of CRF^+ fibers. **I,** Data demonstrating a significant and reversible increase in CIN firing frequency during optogenetic stimulation, *$p < 0.05$, ***$p < 0.001$ by one-way RM ANOVA. n = 13 neurons from 8 animals.

Figure 6. Acute Alcohol Exposure Attenuates CRF-Induced Enhancement of CIN Activity

A, Time course of spontaneous firing in CINs from dorsal striatal slices of ChAT-eGFP mice, before, during, and after bath application of alcohol (EtOH; 50 mM). **B,** Summary data demonstrates a significant reduction in CIN firing frequency following alcohol application. $^{**}p < 0.01$ by Mann-Whitney test. n = 6 cells from 4 mice. **C,** Schematic of the experimental design in which striatal slices were pretreated with alcohol (50 mM) for 1 h in an incubation chamber and then washed for 15 min in the recording chamber. CINs were selected for cell-attached electrophysiological recordings, measuring firing frequency for 10 min (baseline), followed by CRF (40 nM) and alcohol (50 mM) bath applications for 10 min each. **D, E,** Data showing spontaneous firing of CINs during baseline (BL), CRF, and alcohol bath application for the control (D) and alcohol pretreated (E) groups. $^{*}p < 0.05$, $^{**}p < 0.01$, $^{***}p < 0.001$ by one-way RM ANOVA. n = 10 cells from 8 mice (10/8) for the control group and 10/7 for the alcohol pretreated group. **F,** Data showing that alcohol pretreatment attenuated CRF-induced enhancement of CIN firing frequency. $^{*}p < 0.05$ by unpaired t-test. n = 10 cells from 8 mice (10/8) for the control group and 10/7 for the pretreated group.

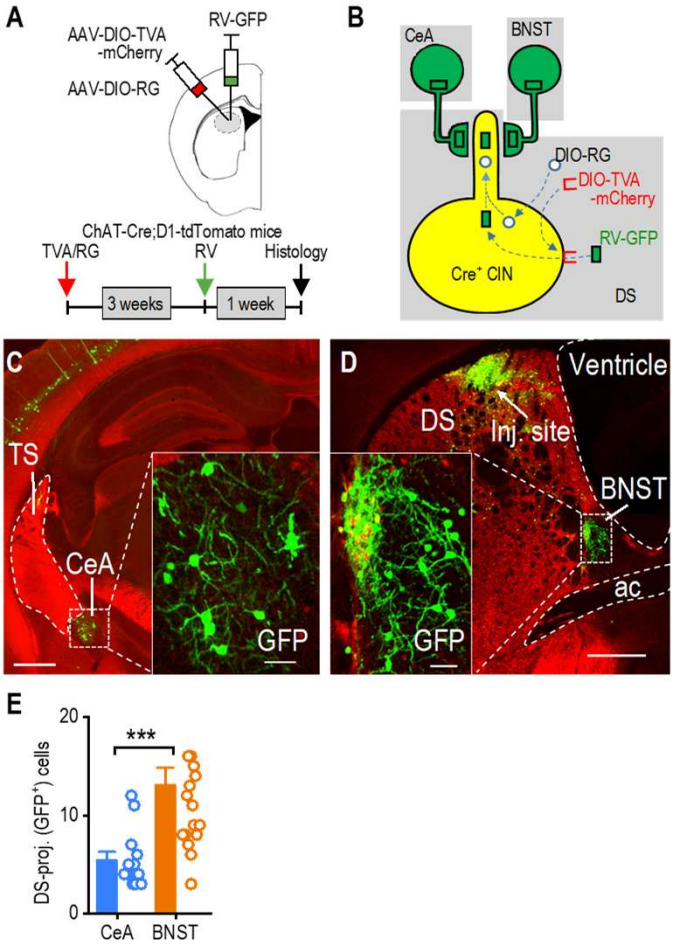
A
AAV-DIO-TVA
-mCherry
RV-GFP
AAV-DIO-RG
ChAT-Cre;D1-tdTomato mice
TVA/RG
RV
Histology
3 weeks
1 week
B
CeA
BNST
DIO-RG
DIO-TVA
-mCherry
RV-GFP
Cre+ CIN
DS
C
TS
CeA
GFP
D
Ventricle
DS
Inj. site
BNST
ac
GFP
E
DS-proj. (GFP+) cells
20
10
0
***
CeA
BNST

Figure 1

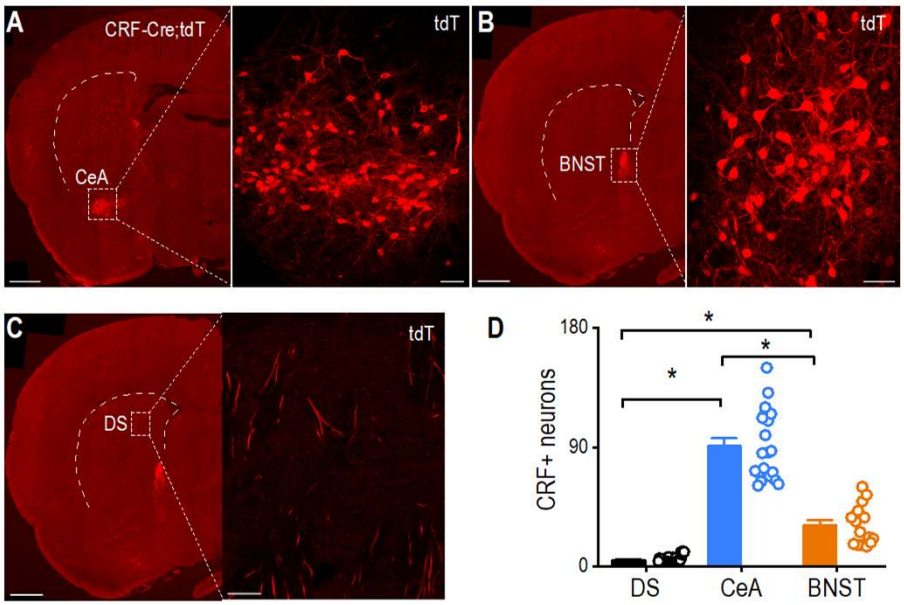
A
CRF-Cre;tdT
CeA
tdT
B
BNST
tdT
C
DS
tdT
D
CRF+ neurons
180
90
0
*
*
*
DS
CeA
BNST

Figure 2

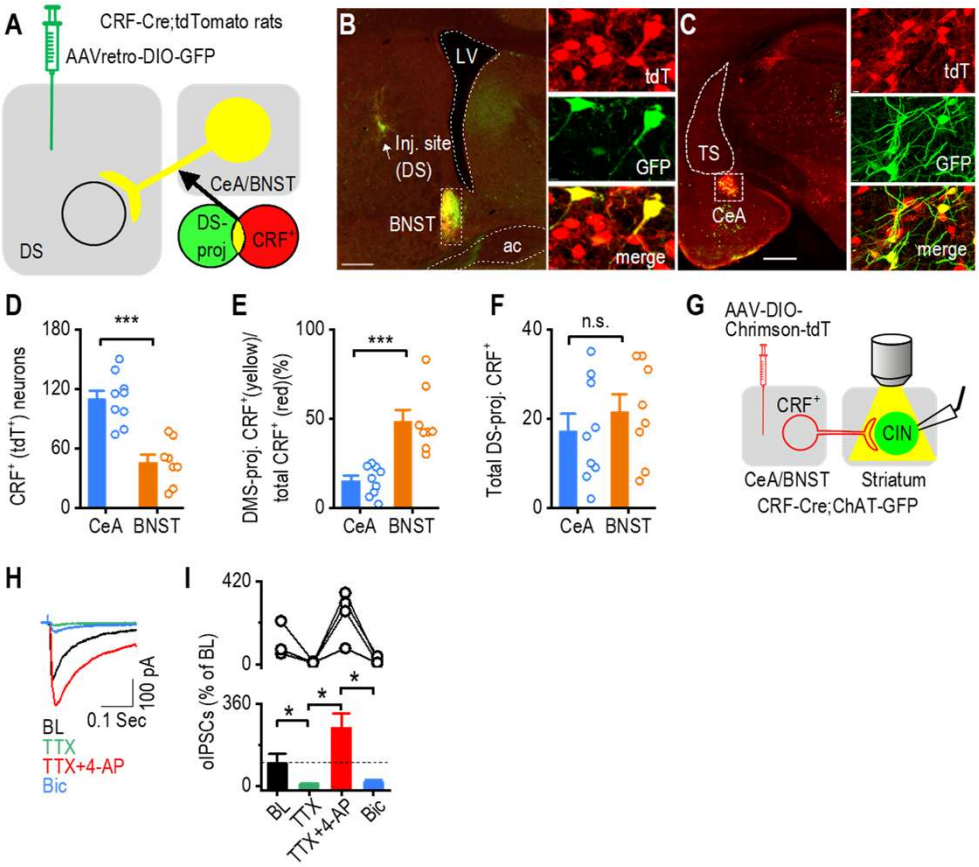
A
CRF-Cre;tdTomato rats
AAVretro-DIO-GFP
CeA/BNST
DS-proj
CRF+
DS
B
LV
Inj. site (DS)
BNST
ac
tdT
GFP
merge
C
TS
CeA
tdT
GFP
merge
D
CRF+ (tdT+) neurons
***
CeA
BNST
E
DMS-proj. CRF+(yellow)/ total CRF+ (red)(%)
***
CeA
BNST
F
Total DS-proj. CRF+
n.s.
CeA
BNST
G
AAV-DIO-Chrimson-tdT
CRF+
CIN
CeA/BNST
Striatum
CRF-Cre;ChAT-GFP
H
100 pA
0.1 Sec
BL
TTX
TTX+4-AP
Bic
I
oIPSCs (% of BL)
BL
TTX
TTX+4-AP
Bic

Figure 3

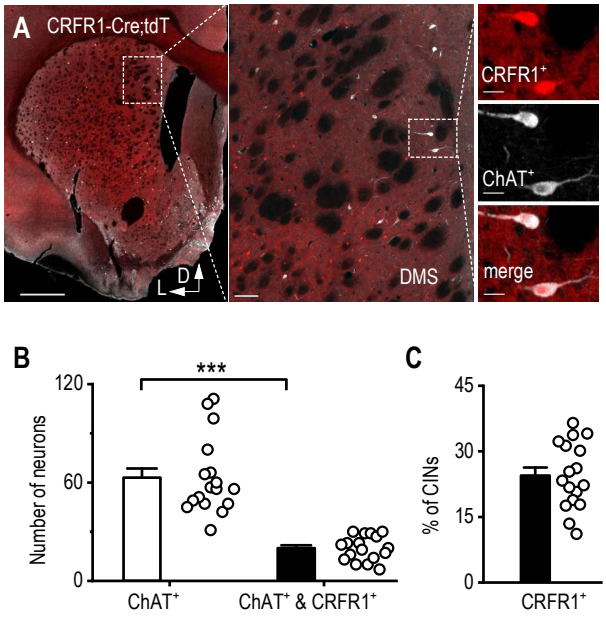
A
CRFR1-Cre;tdT
D
L
DMS
CRFR1+
ChAT+
merge
B
***
120
60
0
Number of neurons
ChAT+
ChAT+ & CRFR1+
C
45
30
15
0
% of CINs
CRFR1+

Figure 4

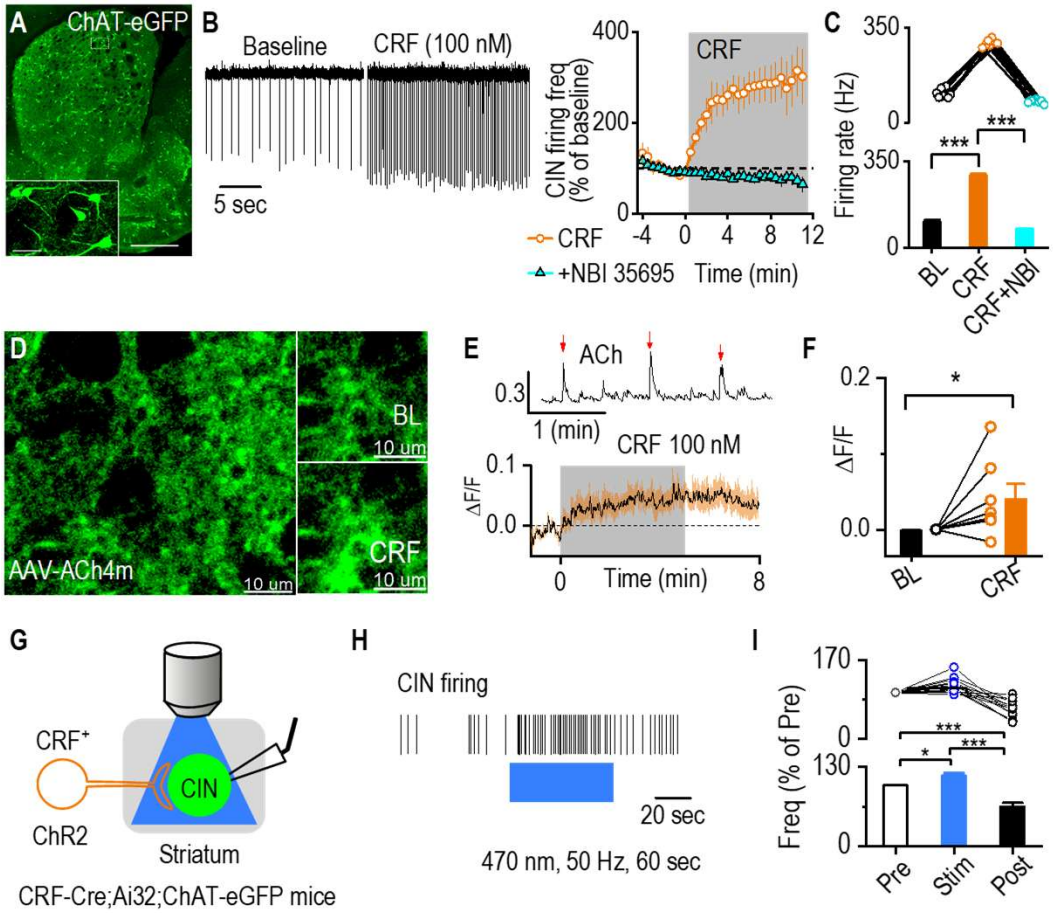
A
ChAT-eGFP
B
Baseline
CRF (100 nM)
5 sec
CIN firing freq (% of baseline)
400
200
0
CRF
-4
0
4
8
12
CRF
+NBI 35695
Time (min)
C
350
0
Firing rate (Hz)
***
***
350
0
BL
CRF
CRF+NBI
D
BL
10 um
CRF
10 um
AAV-ACh4m
10 um
E
ACh
0.3
1 (min)
CRF 100 nM
0.1
ΔF/F
0.0
0
Time (min)
8
F
0.2
*
ΔF/F
0.0
BL
CRF
G
CRF+
CIN
ChR2
Striatum
CRF-Cre;Ai32;ChAT-eGFP mice
H
CIN firing
20 sec
470 nm, 50 Hz, 60 sec
I
170
0
***
*
***
130
0
Freq (% of Pre)
Pre
Stim
Post

Figure 5

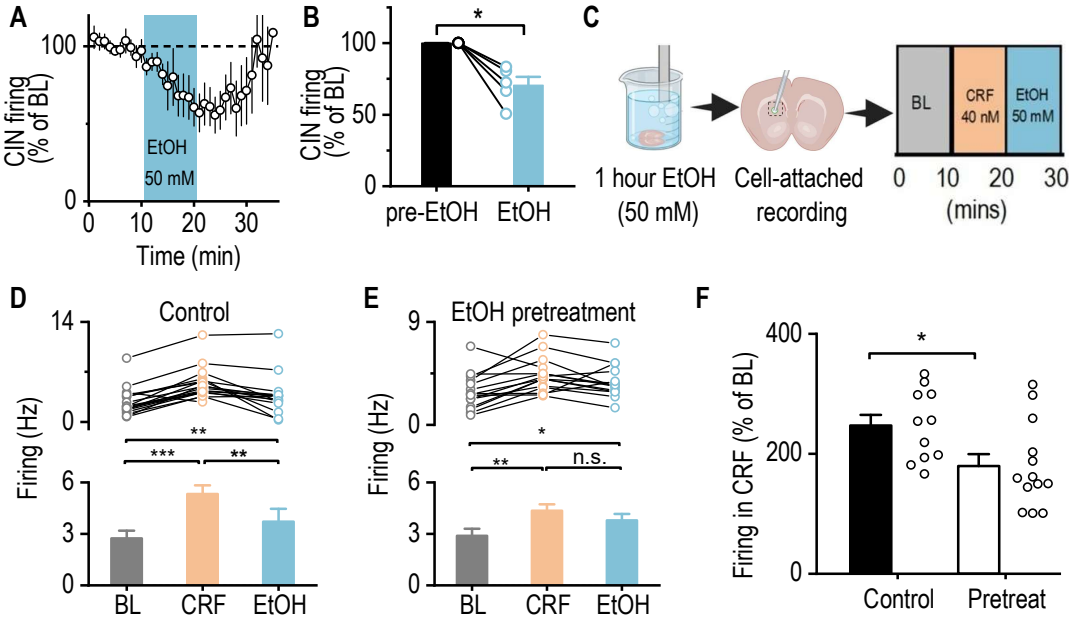
A
100
0
CIN firing (% of BL)
EtOH
50 mM
0
10
20
30
Time (min)
B
*
100
50
0
CIN firing (% of BL)
pre-EtOH
EtOH
C
1 hour EtOH (50 mM)
Cell-attached recording
BL
CRF 40 nM
EtOH 50 mM
0
10
20
30
(mins)
D
Control
14
0
Firing (Hz)
**
***
**
6
3
0
BL
CRF
EtOH
E
EtOH pretreatment
9
0
Firing (Hz)
*
**
n.s.
6
3
0
BL
CRF
EtOH
F
400
200
0
Firing in CRF (% of BL)
*
Control
Pretreat

Figure 6